IAES International Journal of Artificial Intelligence (IJ-AI)
Vol. 15, No. 4, August 2026, pp. 3492~3504
ISSN: 2252-8938, DOI: 10.11591/ijai.v15.i4.pp3492-3504

Image-based estimation of surface roughness in Al-7075 drilling

Shilpa M. Karegoudra, Vamsidhar Yendapalli
Department of Computer Science and Systems Engineering, GITAM School of Computer Science and Engineering, GITAM University, Bengaluru, India

Article Info

Article history:

Received Jun 13, 2025
Revised May 15, 2026
Accepted Jul 9, 2026

Keywords:

Al-7075
Discrete Fourier transform
Discrete wavelet transform
Drilled surface
Gray-level co-occurrence matrix
Non-contact measurement
Surface roughness

ABSTRACT

Surface roughness is an important quality parameter that affects the performance, durability, and reliability of machined components. Measuring the internal surface roughness of drilled holes using conventional contact-based methods is often difficult. Accessibility of the internal surface is complicated due to the diameter of the drilled hole and the need to interrupt the machining process. To overcome these limitations, the proposed work offers a non-contact method for estimating the surface roughness of drilled Al-7075 using image-based analysis. Drilled surfaces are machined using different speeds and feed rates. High-resolution images of the drilled surface are captured using a custom-built image-capturing setup. Texture and frequency features were extracted using gray-level co-occurrence matrix (GLCM), discrete Fourier transform (DFT), and discrete wavelet transform (DWT) techniques. Surface arithmetic average roughness (Ra) was measured using these extracted features. The estimated roughness parameters were then validated by comparing them against roughness parameters obtained by means of the contact stylus technique. According to the experimental results, the accuracy of the wavelet technique is higher, with mean absolute errors of 0.32 μm compared to those obtained using GLCM and DFT techniques. The findings demonstrate that the proposed image-based framework is a reliable and practical solution for non-destructive surface roughness prediction.

Corresponding Author:

Shilpa M. Karegoudra
Department of Computer Science and Systems Engineering
GITAM School of Computer Science and Engineering
GITAM University, Bengaluru, India
Email: skaregou@gitam.in

1. INTRODUCTION

Surface roughness is one of the important quality characteristics of the manufactured parts, and it is directly related to friction, wear, fatigue strength, sealing, and lubrication. Surface roughness measurement is an important task in precision manufacturing industries like aerospace and automotive for the dimensional accuracy and mechanical assembly reliability requirements of the machined parts to meet the design requirements [1]–[3]. The most commonly used measure of surface roughness, the arithmetic average roughness (Ra), is defined as the average of the absolute values of the deviations of the surface profile from a reference line, as shown in Figure 1 for the evaluation length Lm. In industry, Ra is used systematically because it has a good correlation with functional performance requirements and is simple to work with [4]. The development of surface roughness estimation techniques can be seen in Figure 2, which shows that surface roughness estimation techniques have evolved from contact-based methods to in-machine methods.

During drilling, the resulting surface roughness depends on several interacting factors, including cutting speed, feed rate, tool structure, tool wear, and vibration, which prior studies have categorized into setup, operational, and process factors [5]. Surface roughness of the drilled components is of importance in dimensional accuracy, fatigue strength, and general structural behavior under working load [6], [7]. Contact-based stylus profilometers are the standard method for quantifying surface roughness, but they have notable limitations on internally drilled surfaces: accessibility is restricted by hole diameter and depth, measurement often requires interrupting the process or destructively sectioning the workpiece, the stylus can damage the surface, and the method is unsuitable for in-process or real-time monitoring, besides being time-consuming. These constraints motivate the development of reliable non-contact surface roughness estimation methods [8]–[10].

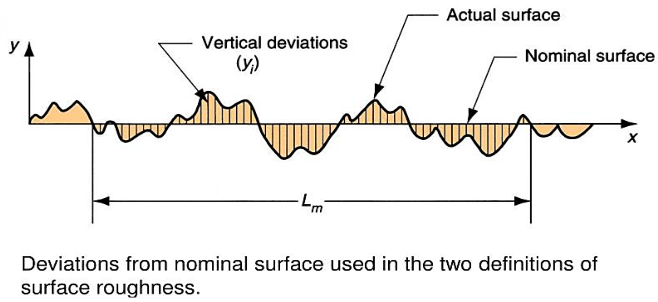

Figure 1. Surface roughness as vertical deviations from the nominal surface

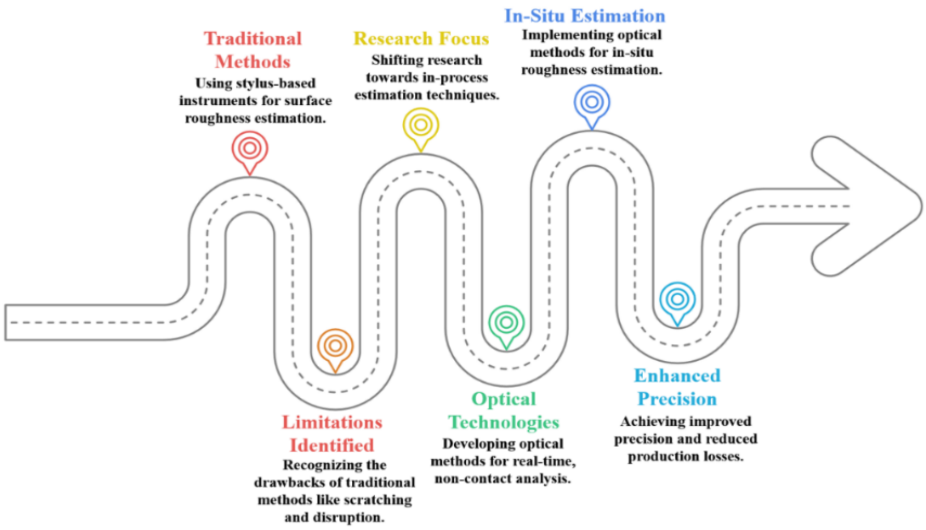

Figure 2. Advancing in surface roughness estimation techniques

To overcome these drawbacks, many studies have been conducted on non-contact surface roughness measurement, especially optical and vision-based approaches, which can rapidly measure the surface roughness without destroying the sample and are compatible with automated surface inspection systems such as laser-based methods, optical coherence tomography (OCT), speckle imaging, and optical surface profiling, as mentioned in [11]–[13]. Of these, image-based estimation has become a viable alternative because it is cost-effective and flexible, and is able to analyze the variations in grayscale intensity and the patterns of texture in the image to obtain the features associated with the roughness. Initial works revealed that some statistical values like standard deviation, variance, and mean of the pixel intensities are correlated with surface roughness in the machined surface [14]. These gray-level co-occurrence matrix (GLCM) features has been used widely for surface texture analysis in turning and milling operations because it captures the spatial relationships between neighbouring pixels, and have been successfully applied for surface texture analysis in turning and milling operations [15]. A vision-based approach to estimate surface texture of milled surfaces based on statistical features of the image [16], [17].

Frequency domain methods have also been explored, such as using the discrete Fourier transform (DFT), which decomposes the spatial frequency components to detect dominant features related to roughness. However, frequency domain analysis is not localizable and may not be sufficient to describe complex Surface features caused by the dynamics of the machining process. Furthermore, all the existing image-based non-contact roughness estimation studies [18]–[20] refer to planar or open surfaces, such as turned, milled or ground parts.

Machine learning and AI-based methods have also been suggested for surface roughness prediction [21]–[24] which are generally based on machining parameters or signals from vibrators, acoustic emission or power consumption sensors. They are effective, but a large training set is necessary, multiple sensors need to be used and they need to be calibrated for each process, and they do not directly investigate the surface texture, so they are not directly applicable to other materials and surface finishes. The wavelet-based analysis is a powerful multi-resolution surface roughness estimation method, which decomposes an image into sub-bands of different frequency spectrum and orientation, and has been found to have good correlation with surface roughness parameters in milling, micromachining and electrical discharge machining (EDM) processes [25], [26]. Wavelet-based image analysis is also limited in its use for the estimation of surface roughness of internal drilled surfaces, with validation against contact-based measurements in a systematic approach.

This paper presents a non-contact image-based method to estimate surface roughness of drilled Al-7075 parts, based on high-resolution images acquired by a custom setup that is designed to be repeatable under different machining conditions [27] to address this. The proposed system explores and compares three feature extraction methods from images, namely GLCM, DFT, and DWT in a systematic manner. The texture and frequency domain features are obtained by these methods and correlated with the values obtained by surface profiler on a stylus-based contact profiler. The reference value is used as the arithmetic Ra parameter, and the performance in estimating the Ra is quantitatively measured by standard error metrics.

2. MATERIAL PREPARATION AND DATA COLLECTION

2.1. Materials preparation

Aluminum is a common substantial in aircraft manufacturing. Different grades of aluminum are used in industry, such as Al-6061 and Al-7075. Al-7075 is the most used material in the industry. Aluminum is a special material because it creates a metal oxide layer that prevents metal from undergoing rusting. Al-7075 is an aluminum alloy that mainly consists of aluminum, along with approximately 5.6–6.1% zinc, 2.1–2.5% magnesium, and 1.2–1.6% copper. It also contains trace amounts (less than 0.5%) of elements such as silicon, iron, manganese, titanium, chromium, and others. The detailed composition is provided in Table 1.

A computer-aided design (CAD) model of drilled Al-7075 plate with dimensions 102×102×25 mm was developed for the study. Drilling operations were carried out using an 8 mm diameter carbide-tipped drill bit. The experiments were performed on an Al-7075 aluminum plate of the same dimensions. Different machining speeds and feed rates were used, including spindle speeds of 2000, 2500, 3000, 3500, and 4000 revolutions per minute (RPM), and feed rates of 25, 50, 75, 100, 125, and 150 mm/min. For each cutting speed, different feed rates were applied. Figure 3 illustrates the complete experimental workflow starting from the computer numerical control (CNC) machine setup used for precision drilling operations, followed by the CAD model of the Al-7075 plate. It continues with the actual drilling process and concludes with the final appearance of the drilled aluminum workpiece, which was later analyzed for surface roughness.

Table 1. Chemical composition of Al-7075 alloy

Compositions	Percentage of content (%)
Aluminum (Al)	90
Zinc (Zn)	5.6
Manganese (Mg)	2.5
Copper (Cu)	1.6
Chromium (Cr)	0.23

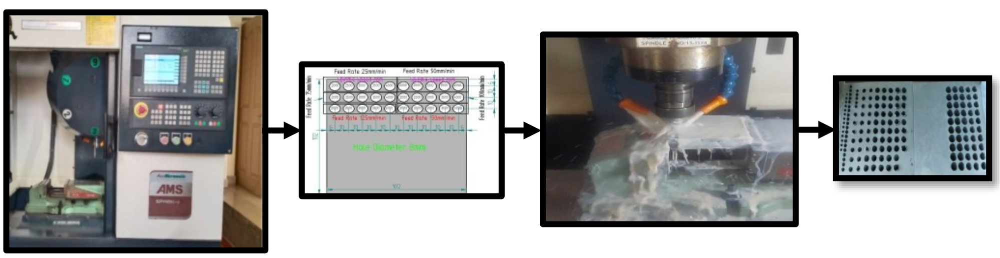

Figure 3. The sequence of steps in material preparation and drilling of the Al-7075 workpiece

2.2. Generation and collection of the dataset for surface roughness estimation

A special image acquisition system was designed to collect a comprehensive set of data to estimate surface roughness. The images required for estimating surface roughness were taken with the help of this specially designed and constructed device. The collected images were then subjected to analysis for determining their surface roughness values.

A specially built rotating-stage imaging apparatus, as illustrated in Figure 4, was utilized, allowing controlled angle measurements at different hole sizes and feed rates. This versatile arrangement provides reliability and strength under various machining conditions. In the case of through holes, no artificial light source is required because the specimen holder is transparent, and ambient light can be utilized for image acquisition.

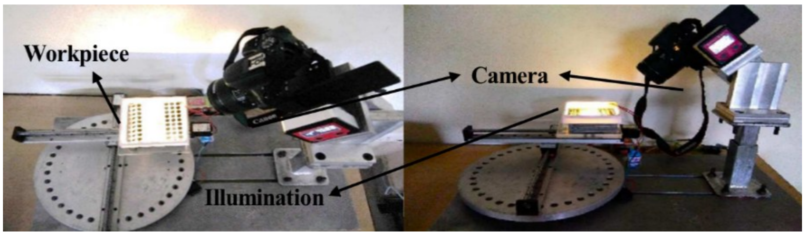

Figure 4. Image capturing setup to capture drilled surface images

The images captured for different diameter holes at different speeds and feeds without illumination are shown in Table 2. The roughness value of the sectioned Al-7075 was measured using the contact method. The device employed for this measurement is the Taylor Hobson surface profiler. It features a stylus tip connected to a probe, which is linked to a controller that displays the roughness value directly. Additionally, the device can be connected to a laptop to obtain a more detailed result, including the stylus travel and the resulting graph. The stylus travels a distance of 4 mm to provide the roughness value. Figure 5 illustrates the device used for measuring roughness using the Taylor Hobson surface profiler. Surface roughness measurements obtained using the Taylor Hobson profilometer follow conventional Ra-based assessment practices consistent with ISO 4287/4288 surface texture evaluation standards. The Ra parameter was selected because of its widespread industrial acceptance and relevance in machining quality assessment.

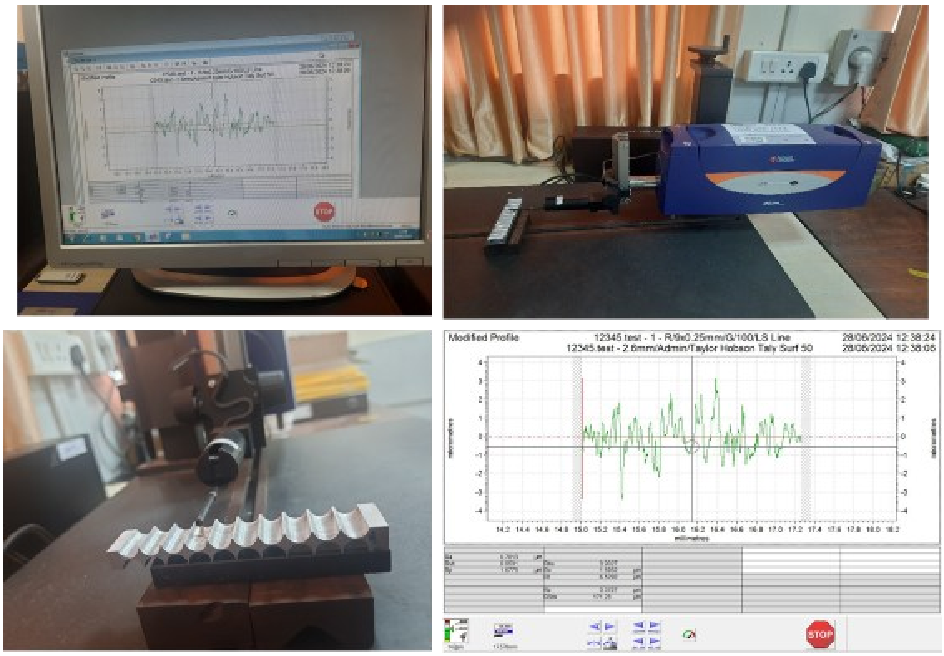

Figure 5. Estimation of surface roughness using a stylus-based Taylor Hobson surface profiler

Table 2. Sample images captured using a custom-built image-capturing setup

Sl No	Feed rate (mm/min)	Spindle Speed (rpm)				
		2,000	2,500	3,000	3,500	4,000
1.	25			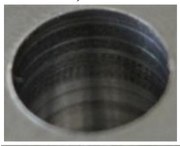		
2.	50	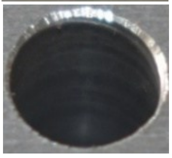	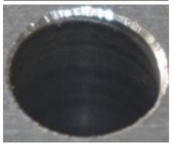	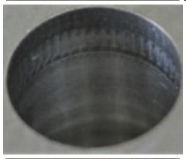		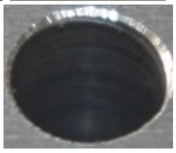
3.	75	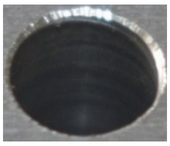	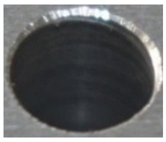	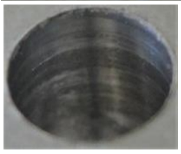	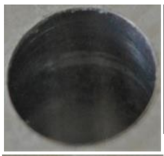	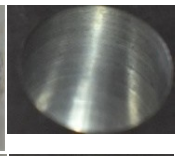
4.	100	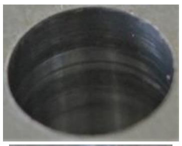		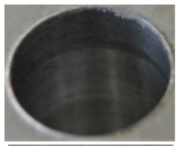		
5.	125					
6.	150		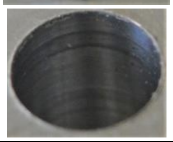			

3. METHOD

This work explores three image-texture-based approaches, like GLCM, DFT, and DWT, to estimate the surface roughness of the drilled surface, as illustrated in Figure 6. The proposed framework demonstrated stable performance under the selected preprocessing configuration (median filter size = 5 and Daubechies wavelet (db4)); however, systematic sensitivity analysis for different preprocessing parameters remains part of future investigation. The methodology is organized into data acquisition, preprocessing, feature extraction, and evaluation steps.

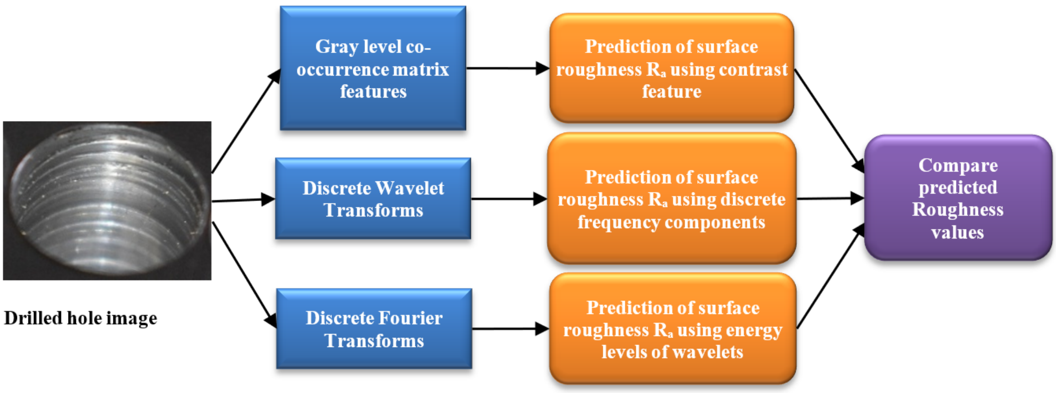

Figure 6. Proposed method workflow diagram

3.1. Data acquisition and preprocessing

Grayscale images of machined surfaces were captured using a custom-built image-capturing setup. The images were then processed and resized using the median filter technique with a kernel size of 5 pixels. Each surface image has a corresponding value of Ra determined using the profilometer, and this serves as the ground truth value. Fuzzy inference systems may also be considered for handling uncertainties due to varying light conditions and noise levels in the images.

3.2. Image preprocessing and feature extraction using gray-level co-occurrence matrix

The captured images of holes were subjected to a series of image processing operations in MATLAB to analyze the surface texture and get an estimate of surface finish. The pipeline starts by converting an image to grayscale using grayscale conversion and then median filtering the image to prepare for texture analysis, and then the GLCM is computed to capture the spatial relationship between the neighboring intensities of the pixels in the image. The statistical parameters obtained from the GLCM are then correlated with the roughness parameters obtained from the profilometer to get a quantitative measurement of surface finish. To analyze the drilled surface texture and estimate surface finish, a series of image processing steps was applied to the captured image using MATLAB.

3.2.1. Image acquisition and grayscale conversion

The input image (4-25.JPG) was first read using the read function. As texture analysis does not rely on color information, the image was converted from RGB to grayscale using the rgb2gray function, reducing computational complexity. Median filtering was applied using medfilt2 to reduce image noise while preserving edges, which is important for accurate texture analysis.

3.2.2. Gray-level co-occurrence matrix computation

GLCM is used to extract the features of the input images, computed by the gray matrix function, following the vision-based texture characterization approach adopted in prior surface roughness studies [14]–[16]. GLCMs were generated for two spatial offsets: [2 0] (horizontal) and [0 2] (vertical). These offsets allow analysis of pixel pair relationships in multiple directions, enhancing texture description. GLCM estimates the spatial arrangement of image texture by counting the frequency of occurrence of pixels in a given offset at a specified direction. There are three parameters in GLCM:

– Distance (d): the separation between two pixels.
– Angle (θ): the direction (0°, 45°, 90°, and 135°) in which pixel pairs are considered.
– Number of distinct intensity levels (G): the number of grey levels in the image.

The GLCM matrix is an m*n matrix consisting of the frequency of occurrences of neighboring pixel values. There is one occurrence of the pixel pair (1,1) and two occurrences of pixel pair (1,2), as illustrated in Figure 7.

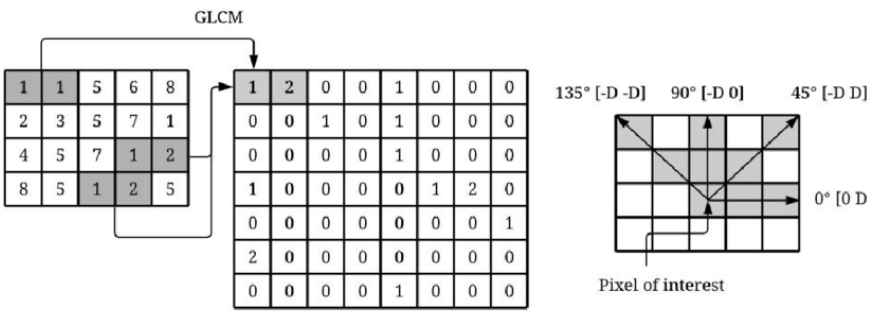

Figure 7. The process used to create the GLCM of the given image

3.2.3. Feature extraction from gray-level co-occurrence matrix

The graycoprops function was used to compute the contrast and correlation features from the GLCMs. Once the GLCM is generated, various features can be extracted to analyze the texture of the image surface. In the proposed system, the contrast feature of the GLCM is extracted to analyze the spatial texture of the surface. The contrast feature indicates the local deviation of pixel distribution in the image. High contrast signifies a greater distance between neighboring pixels. Contrast is calculated as in (1).

$$contrast = \sum_{i,j=1}^{N} P_{i,j}(i-j)^2 \quad (1)$$

Where i, j are the indices of GLCM matrix, and GLCM (i, j) signifies the value at position (i, j) in GLCM.

3.2.4. Surface roughness estimation using gray-level co-occurrence matrix features

In surface roughness estimation, these features quantify how the surface microstructure varies. Among the extracted features, energy is often used as a proxy for roughness since smoother surfaces tend to have more uniform textures (higher energy), while rougher surfaces exhibit more texture variations (lower energy). In this work, energy is directly correlated with the measured surface roughness values obtained from profilometer readings.

3.3. Estimation of the surface roughness using the discrete Fourier transform

DFT and band-pass filters are employed to analyze the surface profile of the drilled surface. The DFT is a mathematical technique used to convert spatial data from the time (or spatial) domain into the frequency domain. For surface roughness analysis, the surface profile, typically a set of height measurements taken at regular intervals, is transformed to identify the frequency components of the surface texture. DFT is given by (2).

$$X_k = \sum_{n=o}^{N-1} x_n \times e^{-i2\pi\frac{k}{N}n} \tag{2}$$

DFT comprises only discrete frequency components. The inverse transform is given in (3).

$$x_n = \frac{1}{N}\sum_{k=o}^{N-1} X_k \times e^{-i2\pi\frac{k}{N}n} \tag{3}$$

Where X_k is the kth frequency element of the DFT with k = 0,1,2... N-1, x_n is the nth sample of the input sequence, i is the imaginary unit, k is the frequency index, n is the sample count, and N is the total number of samples in the sequence.

Steps involved in estimating the surface roughness using DFT and a bandpass filter:

i) Measure the surface profile: use a profilometer to get a series of height measurements.
ii) Apply DFT: the spatial data is transformed into the frequency domain using DFT.
iii) Analyze the frequency spectrum: the frequency components are identified corresponding to different roughness scales.
iv) Band-pass filter: a band-pass filter is used to isolate specific frequency components to focus on certain roughness features.
v) Inverse DFT: the filtered data are converted back to the spatial domain to visualize and analyze the selected roughness features.

3.4. Wavelet-based surface roughness estimation

Surface roughness reflects the micro-scale variations on a material's surface, which can be characterized by analyzing texture patterns in images, as demonstrated for wavelet-based texture descriptors in machined and micromachined surfaces [25], [26]. The wavelet transform provides a powerful multi-resolution tool to extract texture features at different scales and orientations, making it highly suitable for estimating surface roughness from images. Figure 8 describes the steps involved in the procedure.

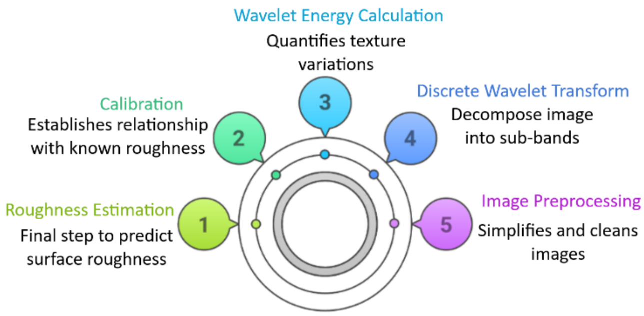

Figure 8. Surface roughness estimation procedure using wavelet transform

3.4.1. Image preprocessing

The raw surface images are first converted to grayscale to simplify analysis and reduce computational complexity. Noise in the images, which can adversely affect feature extraction, is minimized using median filtering. Median filtering helps preserve edges while removing salt-and-pepper noise, ensuring more reliable texture representation.

3.4.2. Discrete wavelet transforms

The core step involves applying the 2D DWT to the preprocessed grayscale image. The DWT divides the image into four sub-bands:
- Approximation coefficients (LL): represent the low-frequency, smooth components of the image.
- Horizontal details (LH): capture horizontal edge and texture details.
- Vertical details (HL): capture vertical edge and texture details.
- Diagonal details (HH): captures diagonal edge and texture details.

The db4 was used as the mother wavelet due to its good localization in both time and frequency domains, which is advantageous for texture analysis. Mathematically, the DWT of an image I can be represented as in (4).

$$DWT(I) = \{LL, LH, HL, HH\} \tag{4}$$

Each coefficient matrix represents image information at different frequency bands and orientations.

3.4.3. Wavelet energy calculation

Surface roughness is associated to the amount of texture or "activity" in the image. This can be quantified by calculating the energy contained in each wavelet sub-band. Energy is computed as the sum of squared coefficients in (5).

$$E_{subband} = \sum_{x,y}(C_{subband}(x,y))^2 \tag{5}$$

Where $C_{subband}(x,y)$ are the wavelet coefficients at location (x,y) in each sub-band (LL, LH, HL, HH). The total wavelet energy is calculated in (6).

$$E_{Total} = E_{LL} + E_{LH} + E_{HL} + E_{HH} \tag{6}$$

Higher energy indicates more texture variations, which generally correspond to higher surface roughness.

3.4.4. Normalization

To make the energy values comparable across images of different sizes, the total energy is normalized by the number of coefficients in the approximation sub-band LL in (7). Where N_{LL} is the number of coefficients in the LL sub-band.

$$E_{norm} = \frac{E_{Total}}{N_{LL}} \tag{7}$$

3.4.5. Roughness estimation and calibration

The normalized energy E_{norm} acts as a feature that correlates with the actual surface roughness values measured by a profilometer. To establish a quantitative relationship, a calibration step is performed by fitting a linear regression model between E_{norm} and known roughness values Ra, as in (8).

$$R = \alpha \times E_{norm} + \beta \tag{8}$$

Where α and β are regression coefficients determined during calibration.

Once calibrated, the model can predict roughness for new images by computing their normalized wavelet energy and applying the regression equation. Future work may incorporate dimensionality reduction and feature optimization approaches such as principal component analysis (PCA). Feature attribution techniques can also be used to identify the most discriminative roughness-related descriptors.

3.5. Error metrics for surface roughness estimation

To quantitatively assess the accuracy of the surface roughness estimation method, the predicted roughness values are compared with the true roughness values using the following metrics. The mean absolute error measures the average magnitude of errors between the predicted roughness values and the true roughness values. It is given in (9).

$$MAE = \frac{1}{N}\sum_{i=1}^{N}|R_{i\,Pred} - R_{itrue}| \tag{9}$$

Mean squared error (MSE) is calculated as in (10). Where N is the total number of samples (images), R_{ipred} is the predicted roughness value for the ith sample, and R_{itrue} is the true roughness value for the ith sample.

$$MSE = \frac{1}{N}\sum_{i=0}^{N}(R_{ipred} - R_{itrue})^2 \tag{10}$$

4. RESULTS AND DISCUSSION

The texture and structure of the finished surface play a significant role in assessing the quality and reliability of the fabricated product. In the proposed system, the drilled surface is considered to estimate its texture after performing drilling operations with specified machining parameters and drill hole diameter. Surface roughness is predicted using image processing techniques.

4.1. Surface roughness values acquired from the Taylor Hobson stylus-based tool

In the existing method, the surface roughness of the drilled surfaces is estimated using the contact method. The Taylor Hobson stylus-based tool is used to estimate the surface roughness of the drilled holes used in the proposed system. Figure 9 shows the results of the drilled surface machined at a speed of 2000 RPM and feed = 30, 35, 40, 45 mm/min for a diameter of 4 mm. Experimental observations indicate that higher feed rates generally increased surface roughness due to increased tool-workpiece interaction, while higher spindle speeds tended to improve surface finish under stable cutting conditions.

In this study, surface roughness values of drilled hole images were estimated using three different image processing approaches: GLCM, DFT, and DWT. The performance of each method was quantitatively evaluated by comparing the estimated Ra values against the benchmark measurements obtained through a contact stylus profilometer. Figure 10 presents the 3D pseudo profiles and surface topography visualizations generated from the grayscale images. These visualizations were generated from the grayscale images, as shown in Figure 10(a). This shows the raw grayscale image of the drilled surface used for texture and intensity analysis. The central line is used to create the appearance of a profile trace resembling a stylus path. Figure 10(b) generated using the grayscale value of the pixels on the center line, this profile is used to represent a surface as per the conventional method for measuring surface roughness. Figure 10(c) shows a 3D visualization of the surface created using the grayscale pixel value indicating surface height. These profiles illustrate the spatial variation in pixel intensity, which correlates with the surface's physical texture. While the numerical prediction methods (GLCM, DFT, DWT) quantify this deviation using statistical and frequency-based features, the 3D pseudo-profile provides a visual representation of these deviations at the pixel level. Peaks and troughs are easily distinguishable in the 3D plots, offering an intuitive understanding of texture severity and spatial distribution.

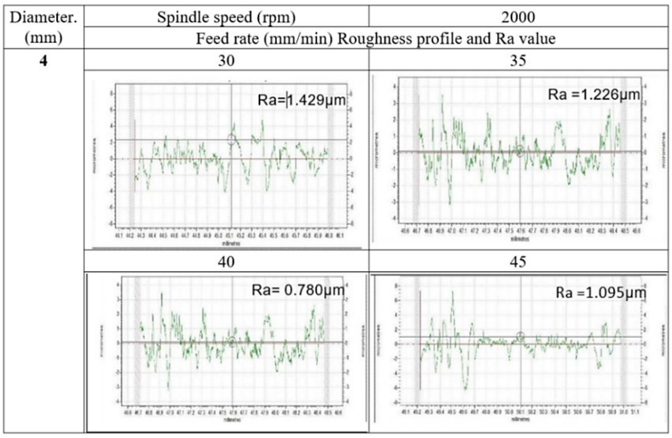

Figure 9. HandySurf results of the drilled and machined surface

4.2. Surface roughness values predicted using GLCM, DFT, and wavelet transform

Surface roughness values predicted using the wavelet transform are shown in Figure 11. Figure 12 shows the DFT-based surface roughness estimation: original grayscale image of the drilled surface, magnitude spectrum of the DFT, and band-pass filtered image highlighting mid-frequency texture features. Statistical parameters such as mean, standard deviation, and root mean square were extracted from the filtered image to estimate surface roughness.

Figure 13 presents a comparative analysis of surface roughness values obtained from the contact method (profilometer) and three non-contact image-based techniques: GLCM, DWT, and DFT. Each bar group represents a different set of machining parameters. As observed, the wavelet transform consistently yields values closest to the contact method, reflecting its superior approximation of true surface texture. This comparison highlights the robustness of wavelet-based approaches in accurately estimating roughness from image data, aligning well with profilometric measurements.

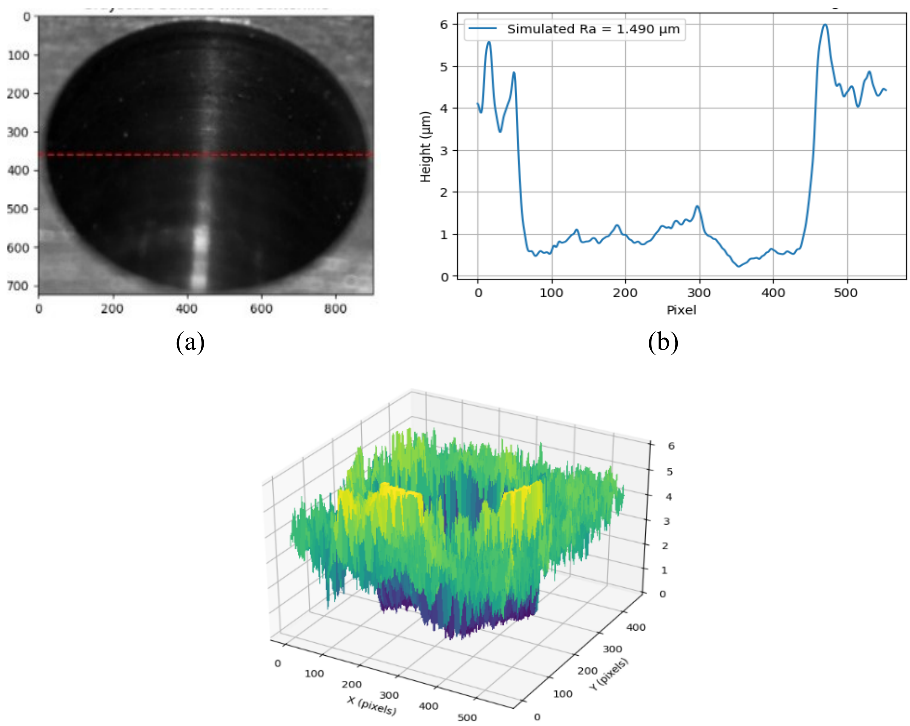

(a) (b)

(c)

Figure 10. 3D presentation of drilled surface: (a) grayscale image, (b) pseudo surface profile, and (c) pseudo surface topology 3D

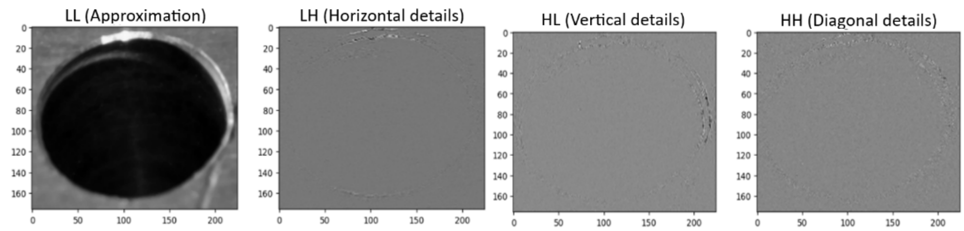


```
Estimated surface roughness: [1.07697493]
Energy in LL: 1447246936.1727057
Energy in LH: 40678.32557162024
Energy in HL: 22647.911441053388
Energy in HH: 9366.50857863934
Mean absolute error: 0.3430250666954635
Mean squared error: 0.1176661963814271
```

Figure 11. Results of the wavelet transform method to estimate surface roughness

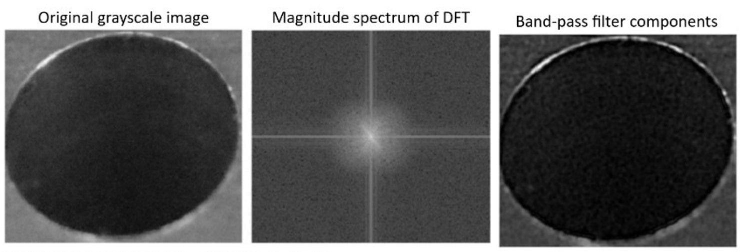


```
Estimated roughness (Std): 0.1044
Estimated roughness (Mean): 0.1360
Estimated roughness (RMS): 0.1715
Estimated roughness (Var): 0.0109
Estimated roughness (MAD): 0.0351
Combined roughness estimate: 0.9158
```

Figure 12. Results of DFT to estimate surface roughness

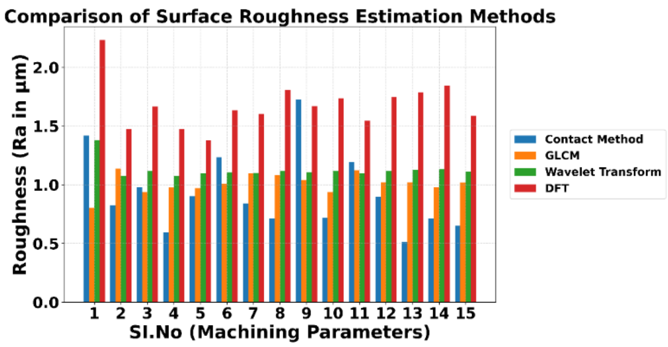

Figure 13. Comparative analysis of image-based surface roughness estimation methods

The experimental results are interpreted in view of the existing studies on surface roughness [10], [18]–[20], [23], [27]. Most reported non-contact roughness prediction methods mainly use machining parameters like spindle speed, feed rate, and tool condition as inputs to learning models, and do not use direct surface image analysis. Image-based non-contact methods in the literature are primarily restricted to planar or open surfaces, such as milled and ground components, where illumination and accessibility of the surface are rather simple. For drilled hole surfaces, several studies have been mainly conducted in contact-based profilometry or indirect analysis by drilling parameters and tool wear, with very few works conducted on image-based or machine learning-based non-contact estimation. In this context, the similarity of the wavelet-based approach with the contact measurements that were observed in this study implies that it is effective in representing the multi-scale surface features of drilled hole interiors that are not well represented by spatial or frequency-only features such as GLCM and the DFT. Explainable artificial intelligence techniques such as Shapley additive explanations (SHAP) and local interpretable model-agnostic explanations (LIME) can further improve interpretability by identifying dominant image features influencing roughness prediction.

Although the present study primarily focuses on image-feature correlation with roughness estimation, the extracted texture and frequency-domain features can also serve as effective inputs to supervised machine learning models such as support vector machines (SVM), random forests (RF), and convolutional neural networks (CNNs). Preliminary observations indicate that wavelet-derived features exhibit strong discriminative capability for data-driven roughness prediction. Integration of intelligent learning frameworks will be considered in future work for improving prediction robustness and scalability.

5. CONCLUSION

This work provided a non-contact image-based framework for the roughness measurement of drilled Al-7075 components. It addresses the problems of non-contact methods in the measurement of internal drilled surfaces through the contact measurement technique. Texture and frequency domain features were extracted from drilled hole images using GLCM, DFT, and DWT methods, and the calculated roughness values were compared with stylus-based profilometer measurements. Experimental results showed that the wavelet-based method gives the best agreement with contact measurement, which has a good estimation accuracy, more than the GLCM and the DFT methods. The proposed framework is a reliable, non-destructive alternative for the analysis of surface roughness and is suitable for applications where accessibility and process interruption are important concerns. Future work will include validation on additional engineering materials such as Al-6061 and steel alloys to evaluate the generalizability of the developed framework across different machining environments and larger datasets. Adaptive imaging systems based on reinforcement learning may further optimize illumination and camera positioning for robust feature acquisition. The proposed framework can potentially be integrated with CNC machine vision systems for real-time in-process surface quality monitoring. and further improve it by combining it with real-time image acquisition and intelligent models for in-line surface quality monitoring in smart manufacturing and Industry 4.0 environments.

ACKNOWLEDGMENTS

The authors would like to acknowledge the valuable contribution of Dr. Veeresha R. K., associate professor of Department of Robotics and Artificial Intelligence, NMAM Institute of Technology, Nitte, for

his expertise in machine learning, image processing, robotics, and artificial intelligence. His continuous guidance was instrumental in the drilling of the workpiece, sectioning the workpiece using the EDM machine, and measuring surface roughness values using the stylus-based contact method.

FUNDING INFORMATION

The authors state no funding is involved.

AUTHOR CONTRIBUTIONS STATEMENT

This journal uses the Contributor Roles Taxonomy (CRediT) to recognize individual author contributions, reduce authorship disputes, and facilitate collaboration.

Name of Author	C	M	So	Va	Fo	I	R	D	O	E	Vi	Su	P	Fu
Shilpa M. Karegoudra	✓	✓	✓	✓	✓	✓	✓	✓	✓	✓			✓	
Vamsidhar Yendapalli		✓			✓	✓		✓		✓	✓	✓	✓	

C : **C**onceptualization	I : **I**nvestigation	Vi : **Vi**sualization
M : **M**ethodology	R : **R**esources	Su : **Su**pervision
So : **So**ftware	D : **D**ata Curation	P : **P**roject administration
Va : **Va**lidation	O : Writing - **O**riginal Draft	Fu : **Fu**nding acquisition
Fo : **Fo**rmal analysis	E : Writing - Review & **E**diting	

CONFLICT OF INTEREST STATEMENT

Authors state no conflict of interest.

INFORMED CONSENT

All authors have given informed consent for publication of this work.

DATA AVAILABILITY

Derived data supporting the findings of this study are available from the corresponding author, [SK], on request.

REFERENCES

[1] A. M. Khorasani, M. R. S. Yazdi, and M. S. Safizadeh, "Analysis of machining parameters effects on surface roughness: a review," *International Journal of Computational Materials Science and Surface Engineering*, vol. 5, no. 1, 2012, doi: 10.1504/IJCMSSE.2012.049055.

[2] T. A. Ruzova and B. Haddadi, "Surface roughness and its measurement methods - Analytical review," *Results in Surfaces and Interfaces*, vol. 19, May 2025, doi: 10.1016/j.rsurfi.2025.100441.

[3] K. Z. Teh, S. Medya, S. Shanmuganathan, and S. H. Yeo, "Review of surface measurement methods towards nondestructive internal surface assessment," *Advanced Manufacturing*, vol. 1, no. 1, 2023, doi: 10.55092/am20230003.

[4] M. Dashti and A. Albannai, "A review on surface roughness (Ra) ranges for some finishing processes," *International Journal of Scientific & Engineering Research*, vol. 11, no. 4, pp. 623–629, 2020.

[5] J. V. A.-Nebot, C. V. Pastor, and H. R. Siller, "A review of the factors influencing surface roughness in machining and their impact on sustainability," *Sustainability*, vol. 16, no. 5, Feb. 2024, doi: 10.3390/su16051917.

[6] A. G. David, V. S. Ramalingam, A. P. Chandran, A. Ramachandran, and A. Selvam, "Statistical modelling and assessment of surface roughness in drilling of hybrid fiber composite," *Multidisciplinary Science Journal*, vol. 6, no. 2, Jul. 2023, doi: 10.31893/multiscience.2024019.

[7] Y.-F. Lin, P.-Y. Lai, G.-Y. Chen, and Z.-P. Zhang, "Optimization of surface roughness and cylindricity using the Taguchi method in boring of S45C steel with tungsten steel and phosphor bronze damping materials," *The International Journal of Advanced Manufacturing Technology*, vol. 135, no. 11–12, pp. 5999–6015, Dec. 2024, doi: 10.1007/s00170-024-14796-x.

[8] J. Guo *et al.*, "Internal surface finishing and roughness measurement: a critical review," *Chinese Journal of Aeronautics*, vol. 38, no. 8, Aug. 2025, doi: 10.1016/j.cja.2024.11.013.

[9] Y. Kondo, I. Yoshida, D. Nakaya, M. Numada, and H. Koshimizu, "Verification of characteristics of Gaussian filter series for surface roughness in ISO and proposal of filter selection guidelines," *Nanomanufacturing and Metrology*, vol. 4, no. 2, pp. 97–108, Jun. 2021, doi: 10.1007/s41871-021-00096-5.

[10] S. Karegoudra and V. Yendapalli, "A systematic review on non-contact methods to estimate the surface roughness," *Materials Today: Proceedings*, vol. 100, pp. 75–92, 2024, doi: 10.1016/j.matpr.2023.05.197.

[11] G. Hutiu, A.-L. Dimb, V.-F. Duma, D. Demian, A. Bradu, and A. G. Podoleanu, "Roughness measurements using optical coherence tomography: a preliminary study," in *Seventh International Conference on Lasers in Medicine*, Aug. 2018, doi: 10.1117/12.2282807.

[12] J. M. Ali, H. S. Jailani, and M. Murugan, "Surface roughness evaluation of electrical discharge machined surfaces using wavelet transform of speckle line images," *Measurement*, vol. 149, Jan. 2020, doi: 10.1016/j.measurement.2019.107029.

[13] M. Shao *et al.*, "A review of surface roughness measurements based on laser speckle method," *Journal of Iron and Steel Research International*, vol. 30, no. 10, pp. 1897–1915, Oct. 2023, doi: 10.1007/s42243-023-00930-8.

[14] J. M. Ali and M. Murugan, "Surface roughness characterisation of turned surfaces using image processing," *International Journal of Machining and Machinability of Materials*, vol. 19, no. 4, 2017, doi: 10.1504/IJMMM.2017.10006839.

[15] D. R. Patel and M. B. Kiran, "Vision-based prediction of surface roughness for end milling," *Materials Today: Proceedings*, vol. 44, pp. 792–796, 2021, doi: 10.1016/j.matpr.2020.10.709.

[16] Manjunatha, R. Rajashekar, B. M. Rajaprakash, S. Naveen, and G. Mohan, "Evaluation of surface roughness of machined components using machine vision technique," *International Journal of Engineering Development and Research*, vol. 5, no. 4, pp. 1256–1263, 2017.

[17] S. I. M. Suhail, J. M. Ali, H. S. Jailani, and M. Murugan, "Vision-based system for surface roughness characterisation of milled surfaces using speckle line images," in *2nd International Conference on Advances in Mechanical Engineering (ICAME 2018)*, Oct. 2018, doi: 10.1088/1757-899X/402/1/012054.

[18] R. Binali, H. Demirpolat, M. Kuntoğlu, and H. Sağlam, "Machinability investigations based on tool wear, surface roughness, cutting temperature, chip morphology and material removal rate during dry and MQL-assisted milling of nimax mold steel," *Lubricants*, vol. 11, no. 3, Feb. 2023, doi: 10.3390/lubricants11030101.

[19] M. S. Ullah and N. R. Dhar, "Effects of vegetable oil-based cutting fluid in machining Kevlar composite material," *American Journal of Mechanical Engineering*, vol. 6, no. 2, pp. 54–60, Jun. 2018, doi: 10.12691/ajme-6-2-3.

[20] R. Zamri, M. N. Maslan, M. S. S. Mohamed, L. Abdullah, M. M. Ali, and M. S. Noorazizi, "The study of light effect on surface roughness of metallic surface by using vision system technique," in *Intelligent Manufacturing and Mechatronics (SympoSIMM 2019)*, Singapore: Springer, 2020, pp. 503–512, doi: 10.1007/978-981-13-9539-0_49.

[21] K. Antosz, E. Kozłowski, J. Sęp, and S. Prucnal, "Application of machine learning to the prediction of surface roughness in the milling process on the basis of sensor signals," *Materials*, vol. 18, no. 1, Jan. 2025, doi: 10.3390/ma18010148.

[22] C. Cooper, J. Zhang, Y. B. Guo, and R. X. Gao, "Surface roughness prediction through GAN-synthesized power signal as a process signature," *Journal of Manufacturing Systems*, vol. 68, pp. 660–669, Jun. 2023, doi: 10.1016/j.jmsy.2023.05.016.

[23] S. Karegoudra and V. Yendapalli, "Estimating the surface roughness of a drilled surface using the edge detection technique," in *2023 International Conference on Recent Advances in Information Technology for Sustainable Development (ICRAIS)*, Nov. 2023, pp. 256–259, doi: 10.1109/ICRAIS59684.2023.10367173.

[24] U. M. R. Paturi, S. T. Palakurthy, and N. S. Reddy, "The role of machine learning in tribology: a systematic review," *Archives of Computational Methods in Engineering*, vol. 30, no. 2, pp. 1345–1397, Mar. 2023, doi: 10.1007/s11831-022-09841-5.

[25] D. Grochała, R. Grzejda, A. Parus, and S. Berczyński, "The Wavelet transform for feature extraction and surface roughness evaluation after micromachining," *Coatings*, vol. 14, no. 2, Feb. 2024, doi: 10.3390/coatings14020210.

[26] V. Chebrolu, R. Koona, and R. S. U. Raju, "Machine vision based surface roughness assessment system based on the Internet of Things and contourlet transforms," *International Journal on Interactive Design and Manufacturing (IJIDeM)*, vol. 19, no. 1, pp. 83–98, Jan. 2025, doi: 10.1007/s12008-023-01515-1.

[27] S. Karegoudra and V. Yendapalli, "Design and development of an image-capturing system for the non-contact estimation of drilled surface roughness," *Engineering, Technology & Applied Science Research*, vol. 15, no. 6, pp. 28950–28955, Dec. 2025, doi: 10.48084/etasr.13149.

BIOGRAPHIES OF AUTHORS

Shilpa M. Karegoudra received her B.E. and M.Tech. degrees in Computer Science and Engineering from Visvesvaraya Technological University, Belagavi, India, in 2012 and 2014, respectively. She is currently pursuing a Ph.D. degree in the Department of Computer Science and Systems Engineering, GITAM School of Computer Science and Engineering, GITAM (Deemed to be University), Bengaluru. Since 2015, she has been an assistant professor at NMAM Institute of Technology, Nitte (Deemed to be a university), Karkala, India. She is the author of 12 articles. Her research interests include natural language processing, machine learning, deep learning, surface metrology, and texture analysis. She can be contacted at email: skaregou@gitam.in or Shilpa.m.k456@gmail.com.

Vamsidhar Yendapalli received a Ph.D. degree in Computer Science and Engineering with a specialization in sustainable software models and AI in the domains of agriculture and automotive. He is currently working as a professor and head of the Department of Computer Science and Systems Engineering, GITAM School of Computer Science and Engineering, GITAM (Deemed to be University), Bengaluru, India. He has 24 years of academic experience, with 2 years in IT. He is the author of 18 articles. His research interests include software engineering, artificial intelligence, and machine learning. He can be contacted at email: vyendapalli@gitam.edu.